

Weakly bound buffer layer as a template for metallic nano-clusters growth and film laser-patterning

Elad Gross, Ori Stein, Micha Asscher^{*}

Department of Physical Chemistry and The Farkas Center for Light Induced Processes, The Hebrew University of Jerusalem, Israel

Available online 1 February 2007

Abstract

Growth of metallic nano-clusters and control over their size are critically important for catalysis. Development of film patterning procedures at the nanometer scale has significant impact on future lithography. In this work, we present an approach to grow metallic nano-clusters and control their size using a weakly bound buffer layer as an intermediate substance and a template to control the clusters size at the range 1–15 nm.

The buffer layer was further employed to create a pattern based on a selective laser ablation procedure. A thicker metallic film deposited on top of pre-patterned buffer layer has been demonstrated as a novel patterning technique at the sub-micron to nanometer scale employing a single laser pulse. The thermal stability of metallic structures prepared this way has been studied at temperature up to 1000 K.

© 2007 Elsevier B.V. All rights reserved.

Keywords: Metallic nano-clusters; Film laser-patterning; Buffer layer

1. Introduction

Transition metal clusters are known for decades as the chemically active sites when supported on the surface of a support oxide that compose heterogeneous catalysts [1]. The introduction of STM has enabled close inspection of the correlation between size and shape of the metallic clusters with their catalytic activity and selectivity. In recent years, gold nano-clusters were demonstrated to have unique catalytic activity for low temperature CO oxidation [2,3], but limited to a very narrow size range near 3 nm diameter, otherwise it is inert [3]. The unusual activity of the gold particles is accepted to arise from quantum size effect, defects on the metal-oxide surface and the detailed atomic-level structure of the metallic nano-clusters [4–6].

Since the size of the metallic clusters is often very important for the overall activity of a catalyst, as in the case of gold, it became necessary to define and understand the parameters that dictate thermal stability of these clusters on the solid surface of a support material. Attempts have been made to study their thermal mobility (diffusion) as a function of the support atomic-level structure [7] and to find ways to stabilize them with the

hope to develop sintering resistant catalysts [8]. Model studies under ultra high vacuum (UHV) conditions of supported metallic clusters are typically based on direct evaporation of metal atoms on top of an oxide surface in vacuum. Size distribution and density of clusters are determined this way by the metal evaporation rate (flux) and the substrate temperature [9–12].

An alternative approach has been proposed by Weaver and co-workers to grow clusters via an inert buffer layer–buffer layer assisted growth (BLAG) [13–16]. Evaporation of metal atoms on top of a layer of Xe [7,13,14], amorphous solid water (ASW) [15,16] or CO₂ [17,18] was demonstrated to enable effective control over clusters size and density. In the case of gold, it was shown that clusters grown on ASW layer are more spherical than those grown via the standard direct evaporation method [15].

The buffer layer method has recently been further developed as an alternative patterning method. This was demonstrated when a thicker metallic film of gold or potassium were grown on a Xe layer that subsequently has been patterned using pulsed laser ablation in a pre-determined structure [14,17,19].

In this report, we describe the evolution of the buffer layer technique from a method to grow and determine metallic clusters size in the 1–15 nm range into a novel patterning procedure that is potentially an alternative for photolithography.

^{*} Corresponding author.

E-mail address: asscher@fh.huji.ac.il (M. Asscher).

2. Experimental

The experiments described in this paper were performed in two separate UHV chambers. Detailed description of the two systems was given elsewhere [7,16]. Briefly, both chambers were equipped with gold evaporators consisting of tungsten filament (0.25 mm diameter) wrapped around gold wire (1 mm diameter, 99.9999% pure). Evaporation rates were calibrated using quartz-microbalance. A W26%Re–W5%Re thermocouple spot welded to the sample (or to the sample holder in the case of the Si) provided temperature monitor that enabled control via linear ramp or temperature stabilization at $\pm 1^\circ$ accuracy. Sample cleaning was achieved via ion sputtering (Ar^+/Ne^+ ions, 700 eV) and annealing of the samples. The first chamber was mainly used for the growth of gold nano-clusters using water molecules (deposited as amorphous solid water when deposited at sample temperature below 130 K) as buffer layer, employing BLAG. In this system, $\text{SiO}_2/\text{Si}(1\ 0\ 0)$ samples were attached to a liquid nitrogen Dewar via two tantalum foils, spot welded to copper feed throughs in direct contact with the LN_2 reservoir. After annealing the sample at 700 K, triple-distilled water molecules were introduced by backfilling the UHV chamber, adsorbing on the sample held at 140 K. Following gold atoms deposition, small clusters are formed this way, which are stable up to the ice desorbing temperature. The sample was then slowly heated to 300 K, in order to remove the ASW buffer layer. While the buffer layer evaporated, the gold clusters coalesce and grow. Desorption of the ASW layer led to deposition of the aggregated clusters on the substrate. The sample was then transferred from the vacuum chamber and was imaged at ambient conditions by AFM (DI-3000). Light tapping mode AFM measurements were performed in order to characterize the clusters height. The same sample was subsequently characterized by HR-SEM in order to determine the clusters diameter.

In the second chamber, a $\text{Ru}(0\ 0\ 1)$ sample, 8 mm diameter, 1 mm thick was mounted on a He closed cycle cryostat (ADP Inc.), cooling the sample to 30 K. Base pressure in this chamber was at a level of 4×10^{-10} mbar. Under these conditions Xe (99.9999% pure) was introduced by backfilling the chamber in order to form the buffer layer at thickness in the range 30–200 ML. Standard sample cleaning and characterization procedures

were used as described elsewhere [7]. A grating-like pattern of the Xe layer is formed by splitting a Nd:YAG laser beam (p-polarized, 1064 nm, 10 ns pulse width) with subsequent recombination of the two parts of the beam on the surface, resulting in selective laser induced desorption of the Xe film, as described before [17].

3. Results and discussion

3.1. Nanometer sized clusters grown via BLAG method

In this part, we demonstrate how one can use water as a buffer layer in order to control the size and density of gold nanoparticles on a $\text{SiO}_2/\text{Si}(1\ 0\ 0)$ substrate. Relatively small amounts of gold (up to 1.5 Å, determined by quartz microbalance) were evaporated on various thicknesses of ASW layers grown on top of the $\text{SiO}_2/\text{Si}(1\ 0\ 0)$ sample. AFM images in Fig. 1 demonstrate that both size and density of the gold clusters depend on the amount of evaporated gold and buffer layer thickness. Evaporation of 0.2 Å Au on 10 ML of ASW led to clusters density of $28 \times 10^{10} \text{ cm}^{-2}$ with average clusters height of 0.5 nm. When 1.2 Å Au were deposited on top of 10 ML of ASW, clusters density and height increased to $64 \times 10^{10} \text{ cm}^{-2}$ and 2 nm, respectively (Fig. 1A). By increasing the buffer layer thickness to 100 ML with the same 1.2 Å of gold, the density of clusters decreased to $11 \times 10^{10} \text{ cm}^{-2}$ while their height increased to 4.5 nm (Fig. 1B). By decreasing the evaporated gold amount to 0.4 Å while the buffer layer thickness was kept constant (100 ML), the clusters density was reduced to $8 \times 10^{10} \text{ cm}^{-2}$, while their height decreased to 2.6 nm (Fig. 1C). These results demonstrate how by changing the initial parameters of the BLAG method, clusters height can be changed by an order of magnitude and density can be modified by a factor of 8.

Further examination of the images in Fig. 1 reveals that changes in clusters size are accompanied by changes in clusters size distribution. Small clusters are characterized by a relatively narrow size distribution. In order to calculate the clusters size distribution we have measured the full width at half maximum (FWHM) of the distribution of sizes. The clusters in Fig. 1A are characterized by a FWHM value of 0.1 nm. Increasing the amount of deposited gold from 0.2 to 1.2 Å have lead to the

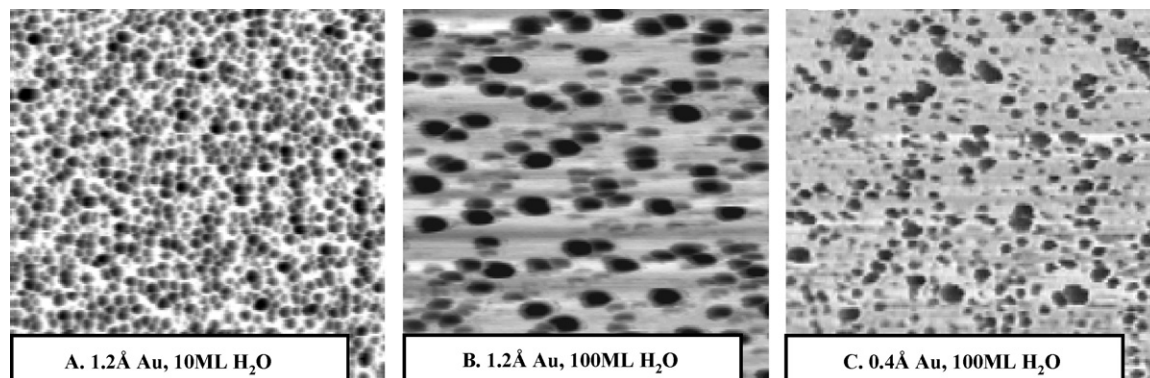


Fig. 1. (A–C) Buffer layer (ASW) assisted growth (BLAG) of gold clusters on $\text{SiO}_2/\text{Si}(1\ 0\ 0)$ substrate held at 130 K. AFM images were taken ex situ at room temperature. The image scale is 500 nm \times 500 nm.

formation of larger clusters and wider size distributions, FWHM = 4.4 nm (Fig. 1B).

Thicker buffer layer lead to larger clusters accompanied by wider distributions, as can be seen in Fig. 1B, where FWHM = 8.5 nm. This behavior can be rationalized by the fact that in order to form higher (larger) clusters, coalescence of two clusters or more must occur. Thicker buffer layer allows longer time for the coalescence process to develop, thus leading to the formation of larger clusters and wider distributions [13]. Increasing the amount of evaporated gold affects both clusters size and density.

We have quantified this tendency by evaporating different amounts of gold on top of 7 ML ASW (Fig. 2A). At small dosage of gold the clusters density grows as the amount of the evaporated gold increases. Clusters density reaches saturation above gold dosage of 1 Å. This phenomenon can be explained assuming that when large enough amounts of gold are deposited, each gold atom that hits the surface of the ASW layer diffuses to the nearest cluster. Increasing the amount of evaporated gold, therefore, will only increase the clusters size but should not influence the density of the initial seed clusters, which means approaching saturation value of clusters density.

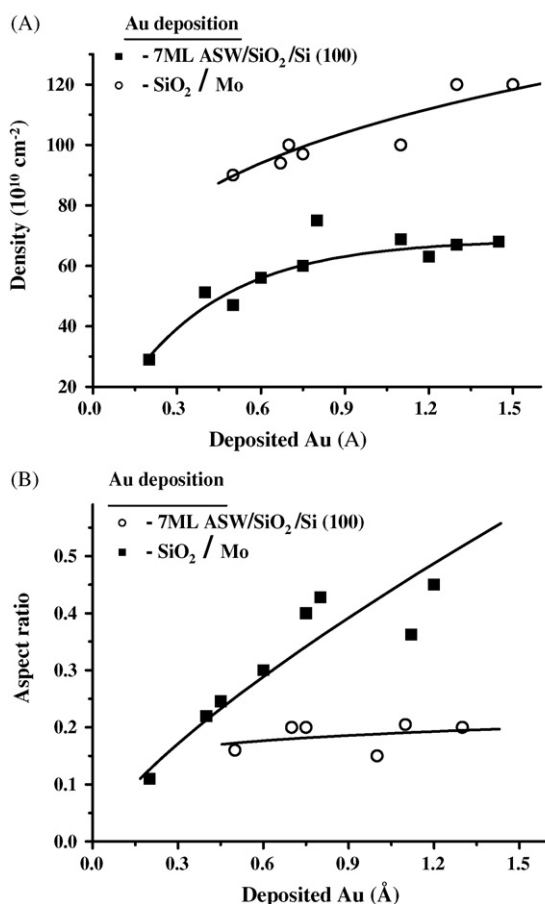


Fig. 2. (A) Density of gold clusters as a function of the amount of deposited gold. Direct deposition (DD) of gold on $\text{SiO}_2/\text{Mo}(1\ 0\ 0)$ substrate is compared with that obtained from the deposition of gold on top of 7 ML of ASW. (B) Aspect ratio (height/diameter) of gold clusters as a function of the amount of deposited gold, for the same substrate as in Fig. 2A.

A more common method for clusters growth practiced in model studies involves direct deposition (DD) of evaporated metal on oxide surfaces. In this method clusters density and size depend on the amount or flux of evaporated metal and the substrate's temperature. We compared between clusters that were grown via the DD method and clusters that were grown using the BLAG approach on top of 7 ML ASW (Fig. 2A). Densities of clusters grown via DD are twice higher than those obtained by the BLAG method. BLAG induced clusters reached density saturation values when more than 1 Å of gold has been evaporated, while densities of clusters prepared by DD have not reached saturation values even at gold dosage more than 1.5 Å. These observations can be rationalized by the fact that 7 ML of buffer layer is too thin to allow aggregation and coalescence during the buffer evaporation [14].

We conclude, therefore, that the difference in clusters size and density between the two deposition procedures arises from differences in diffusion and coalescence rates on the silicon oxide surface versus that on top of the ASW buffer layer. Higher diffusion rates on top of the ASW layer would lead to lower density of seed clusters and subsequently also to a reduced number of clusters on the substrate.

Differences in diffusion rates may also explain the variance in clusters size. For example, clusters produced by DD of 1.2 Å of gold on model SiO_2 grown on Mo substrate [12] had an average height of 0.8 nm, while clusters formed by evaporating the same amount of gold on top of 7 ML ASW as the buffer layer have led to the formation of clusters more than twice higher, with average height of 2 nm.

By combining height analysis (determined by AFM measurements) and clusters diameter (determined by HR-SEM measurements) we have defined the clusters aspect ratio, which is the ratio between clusters average height to its diameter. It is demonstrated that when different amounts of gold are evaporated on 7 ML of ASW, the aspect ratio of the clusters increases with the growth in the amount of evaporated gold. However, the aspect ratio of clusters prepared via the DD method was almost independent of the gold dosage (Fig. 2B).

Clusters grown via the DD method are characterized by a small aspect ratio (0.1–0.2), while the BLAG clusters can reach aspect ratio of 0.5, which means that their structure approaches half sphere.

In conclusion, differences in density, height and aspect ratio between clusters grown by BLAG and DD methods suggest that the DD technique impede coalescence of small clusters on oxide surfaces. Clusters made by direct deposition are characterized by small aspect ratio, therefore are flatter and more 2D in nature than the BLAG grown clusters. These differences suggest that the number and type of catalytically active sites on these clusters should be quite different in terms of yield and selectivity.

3.2. Lift-off laser-patterning using buffer materials

Thicker metal layers (e.g. gold) deposited on top of the buffer material has enabled us to develop a new patterning concept when coupled to selective laser ablation [17,19]. This

patterning procedure utilizes Xe as the weakly bound buffer layer that functions as a template for metal deposition. Following laser ablation, the gold film transforms into metal stripes strongly attached to the surface. The method proceeds as follows: following a standard sputter and anneal procedure, the surface was exposed to 120 layers of Xe at 20 K (calibrated by temperature programmed desorption (TPD) of CO multilayers near 25–30 K). A grating-like patterning of the Xe layer is then formed by splitting a laser beam (50% intensity ratio) and recombining it on the surface, thus creating an interference pattern, which resulted in a sinusoidal temperature profile and in the ablation of the Xe layer from the hot areas. On top of the Xe-grating, 7 ± 1 nm of gold was vacuum-deposited in order to grow a smooth epitaxial film in the Xe depleted areas of the grating. Gold clusters grow on top of the remaining buffer stripes, typical to metal growth on top of buffer layers. Subsequently, a second, uniform and somewhat higher power laser pulse strikes the entire surface in order to remove (ablate) the remaining Xe layer and the gold on top of it, leaving behind gold stripes strongly attached to the ruthenium surface. After producing the gold coverage grating, the sample was slowly heated to 100 K at a rate of 1 K/s in order to desorb residual buffer material still attached to the surface. The gold grating obtained this way was characterized by in situ He-Ne laser diffraction measurements. In addition, ex situ characterization was performed using tapping mode AFM at room temperature.

The interfering laser pulse power was in the range 17–22 mJ/cm² while the second, uniform laser pulse, was 30–60 mJ/cm². These values are all below the damage threshold for the Ruthenium surface. The width of the grating troughs is determined by the (first) laser power absorbed by the substrate. This is due to the exponential dependence of the buffer material desorption rate on substrate temperature. First laser pulse power can be used to vary the width of the Xe grating troughs within a given period; as the power increases, the ablated Xe troughs become wider, giving way to wider gold stripes that are strongly attached to the surface. Fig. 3 demonstrates the control over the width of the gold stripes achieved by adjustments of the

interfering laser power: higher power (23.3 mJ/cm² in Fig. 3A) forms wide Xe and gold stripes, while lower power (18.4 mJ/cm² in Fig. 3B) results in narrower Xe/gold stripes.

The grating period (w) is dictated by the laser wavelength and the incidence angle (φ) between the two interfering beams according to the Bragg equation [20]: $w = \frac{\lambda}{2 \sin(\varphi)}$. Increasing φ shrinks the grating period. For example: setting φ to 32° and first laser pulse of 20.8 mJ/cm² has led to 1.0 μm period with gold line width of 650 nm (not shown). As can be seen from Fig. 3, there are gold clusters, with average height of 35 nm, deposited at the edges of each stripe. These clusters are believed to appear as a result of the preformed buffer layer grating edge profile. The Xe grating gradually becomes less steep at the edges. As a result, a certain ablation power threshold is crossed and the thermal energy delivered to the Xe atoms from the (second) laser pulse is insufficient anymore to ablate the gold layer residing on top.

Few gold clusters are found at the depleted stripes. These clusters were not ejected to the vacuum as a result of the second pulse. These clusters and those at the edges of the gold stripes were found to be rather independent of the second laser pulse with respect to their height and density.

Next we have attempted to study the thermal stability of the gold stripes produced via the lift-off method. Several experiments were carried out in which the gold grating was annealed to 550 and 1000 K at a heating rate of 1 K/s as demonstrated by AFM images in Fig. 4. These images revealed that the gold clusters are totally absent in the clean, depleted areas of the grating. In addition, the clusters at the edges of the gold stripes seem to have decreased in both height and density. This is attributed to diffusion of the clusters in the clean Ru(0 0 1) areas towards the edge of the gold stripes. During anneal of the sample to 550 and 1000 K, we have recorded the first order linear diffraction intensity. Heating to 1000 K results in diffraction signal diminishing down to about 5% of its original intensity, yet the actual gold stripes appearance seems to have been preserved with only minor deterioration of its long range periodicity. In addition, enhanced corrugation at the

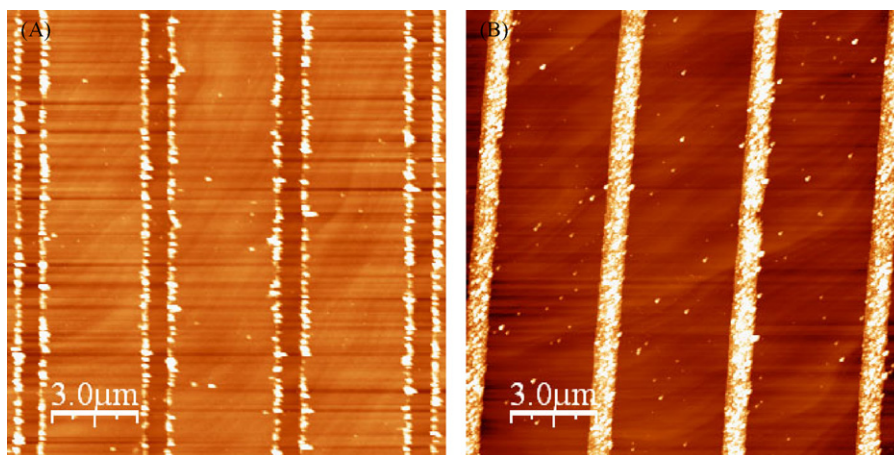


Fig. 3. Gold stripes over Ru(1 0 0) prepared via the buffer layer lift-off method at a fixed grating period (laser wavelength = 1064 nm, angle of incidence = 6.8°). Width of the gold stripes varies by adjusting the first (interfering) laser power. (A) First laser power: 23.2 mJ/cm², wide Xe and gold stripes. (B) First laser power: 18.4 mJ/cm², narrow Xe and gold stripes. In both cases the gold film was 4 ± 1 nm thick (determined by quartz microbalance) and the periodicity was 4.5 μm.

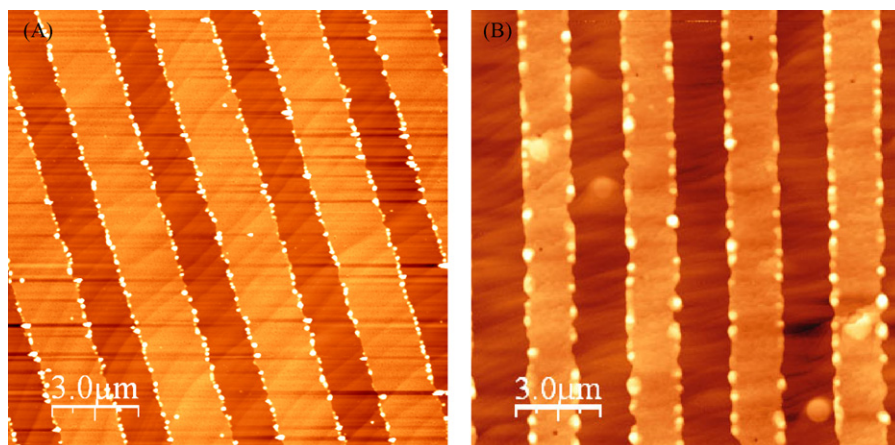


Fig. 4. Thermal stability of the gold grating prepared on Ru(1 0 0). (A) Following heating to 550 K at a heating rate of 1 K/s. (B) Annealing to 1000 K at 1 K/s.

edges of the gold stripes during the annealing process was noted (see Fig. 4), possibly due to melting of the large clusters at the edges and their fusion into the bulk gold stripes.

4. Conclusions

The application of weakly bound buffer layer is demonstrated as a tool for the growth of size controlled metallic nano-clusters on solid surfaces. Thicker metallic films can be utilized in order to pattern the metal/buffer interface in order to form selective metallic structures on practically any substrate. These concepts has been demonstrated for gold nano-clusters growth on SiO₂/Si(1 0 0) using ASW layers as the buffer material. It was demonstrated that as the ASW layer thickness grows, one can obtain larger clusters in the range 3–6 nm, at density in the range $(10\text{--}65) \times 10^{10}$ clusters/cm².

Using 60 monolayers of Xe as the buffer layer and 5–7 nm thick films of gold, grating-like structures of gold were created employing selective laser ablation technique. One could control the width of the metallic stripes down to sub-micron range by changing the ablation laser power. The periodicity of the grating has been determined by the angle of incident between two laser beams and the laser wavelength.

Acknowledgements

This work was partially supported by a grant from the US-Israel Binational Science Foundation and the Israel Science Foundation. The support from The James Frack Program is

acknowledged. The Farkas center is supported by the Bundesministerium für Forschung und Technologie and the Minerva Gesellschaft für die Forschung mbh.

References

- [1] G.A. Somorjai, Introduction to Surface Chemistry and Catalysis, John Wiley, New York, 1994.
- [2] M. Haruta, Catal. Today 36 (1997) 153.
- [3] M. Valden, X. Lai, D.W. Goodman, Science 281 (1998) 1647.
- [4] A. Sanchez, S. Abbet, U. Heiz, W.D. Schneider, H. Hakkinen, R.N. Barnet, U. Landman, J. Phys. Chem. A 103 (1999) 9573.
- [5] N. Lopez, J.K. Nørskov, Surf. Sci. 515 (2002) 175.
- [6] M.S. Chen, D.W. Goodman, Science 306 (2004) 252.
- [7] G. Kerner, Y. Horowitz, M. Asscher, J. Phys. Chem. B 109 (2005) 4545.
- [8] B.K. Kim, W.T. Wallace, D.W. Goodman, J. Chem. Phys. B 108 (2004) 14609.
- [9] C.T. Campbell, Surf. Sci. Rep. 27 (1997) 1.
- [10] C.R. Henry, Surf. Sci. Rep. 31 (1998) 231.
- [11] H.-J. Freund, Angew. Chem. Int. Ed. Engl. 36 (1997) 452.
- [12] S.C. Street, C. Xu, D.W. Goodman, Annu. Rev. Chem. 48 (1997) 43.
- [13] L. Huang, S.J. Chey, J.H. Weaver, Phys. Rev. Lett. 80 (1998) 4095.
- [14] V.N. Antonov, J.S. Palmer, A. Bhatti, J.H. Weaver, Phys. Rev. B 68 (2003) 205418.
- [15] E. Gross, Y. Horowitz, M. Asscher, Langmuir 21 (2005) 8892–8898.
- [16] X.-M. Yan, J. Ni, M. Robbins, H.J. Park, W. Zhao, J.M. White, J. Nanopart. Res. 4 (2002) 525.
- [17] G. Kerner, M. Asscher, Nano Lett. 4 (2004) 1433.
- [18] P.S. Waggoner, J.S. Palmer, V.N. Antonov, J.H. Weaver, Surf. Sci. 596 (2005) 12.
- [19] G. Kerner, M. Asscher, Surf. Sci. 557 (2004) 5.
- [20] X.D. Zhu, Th. Rasing, Y.R. Shen, Phys. Rev. Lett. 61 (1988) 2883.